# All-Optical XOR Using Mach-Zehnder Interferometer

N. K. Dutta[1], Q. Wang[1], G. Zhu[1], H. Chen[1], J. Jaques[2], J. Leuthold[3]

1. Department of Physics, University of Connecticut, Storrs, CT
2. Lucent Technologies, Murray Hill, NJ
3. Lucent Technologies, Holmdel, NJ

## ABSTRACT

All optical XOR functionality has been demonstrated experimentally using an integrated SOA-based Mach-Zehnder interferometer (SOA-MZI) at 20 and 40 Gb/s. The performance of the XOR results has been analyzed by solving the rate equation of the SOA numerically. The high-speed operation is limited by the carrier lifetime in the SOA. In order to solve the limitations imposed by carrier lifetime, a differential scheme for XOR operation has been experimentally investigated. This scheme is potentially capable of XOR operation to > 100 Gb/s.

**Keywords:** Optical logic, Mach-Zehnder Interferometer, Optical amplifier

## INTRODUCTION

It is believed that an ultrafast all-optical exclusive OR (XOR) logic gate is an important component in OTDM communication networks. It can be used in all-optical signal processing such as bit pattern matching [1], pseudo random number generation [2] and label swapping [3]. As is the case for electronic logic gates, all-optical logic gates fundamentally rely on nonlinearities [4]. So far, methods utilizing the nonlinearities of optical fiber[1,5] and semiconductor optical amplifier (SOA)[6,7,8] have been used to demonstrate all optical XOR functionality. The semiconductor optical amplifier has the advantages of high nonlinearity and ease of integration. All optical logic XOR up to 20 Gb/s have been demonstrated with semiconductor optical amplifier (SOA) loop mirror (SLALOM) [6], ultrafast nonlinear interferometer (UNI) [7], and SOA based Mach-Zehnder interferometer (SOA-MZI) [8]. The all-optical logical gate base on SOA-MZI is believed to be stable, compact and simple.

In this paper, all optical logic XOR is demonstrated experimentally at 20 Gb/s and 40 Gb/s with the scheme demonstrated in ref. 8. The performance of XOR gate, especially the pattern dependence is analyzed by solving SOA carrier rate equations numerically. Both the experimental results and simulation results show that the operation speed of all optical XOR is limited by the carrier recovery time of SOA. A differential phase modulation scheme is proposed to solve this limitation. The proposed scheme is demonstrated at 20 Gb/s experimentally, and simulation shows this scheme is potentially capable of XOR operation up to 100 Gb/s.

## EXPERIMENT

The 20 Gb/s data pattern of “1100” is generated by passively multiplexing the gain switched DFB laser pulses with 5 GHz repetition rate, after dividing by 50:50 coupler and delay of 50-ps for one

Active and Passive Optical Components for WDM Communications IV, edited by Achyut K. Dutta, Abdul Ahad S. Awwal, Niloy K. Dutta, Yasutake Ohishi, Proc. of SPIE Vol. 5595 (SPIE, Bellingham, WA, 2004) · 0277-786X/04/$15 · doi: 10.1117/12.583171

pulse train. The pulse width is about 7-ps after pulse compression using a high dispersion fiber, and the center wavelength is 1545 nm. As shown in Figure 1, 20 Gb/s data pattern of "1100" is

split into two data streams, and one (data A) is injected into the control input 1 of the SOA-MZI, and the other (data B) is injected into the control input 2 of the SOA-MZI. The average powers of both data streams are amplified to 10 dBm with erbium doped fiber amplifiers (EDFA). The CW light is provided with another DFB laser at 1557 nm, it is also amplified to 10 dBm before it is sent into the port 3 of the SOA-MZI. After cross-phase modulation in the SOA-MZI, the wavelength-converted output signal at 1557nm is coupled out of port 4, where a filter selects the converted signal before it is observed using a 30 GHz sampling oscilloscope. It is noted that the high power is needed due to the high insertion loss of the SOA-MZI (>10 dB at both sides). For the generation of 40 Gb/s data pattern, the experimental set up is same as shown in Figure 1 except the modulators are driven at 10 GHz and the optical delays are appropriately reduced. For the principle of all optical logic XOR, see ref. 8.

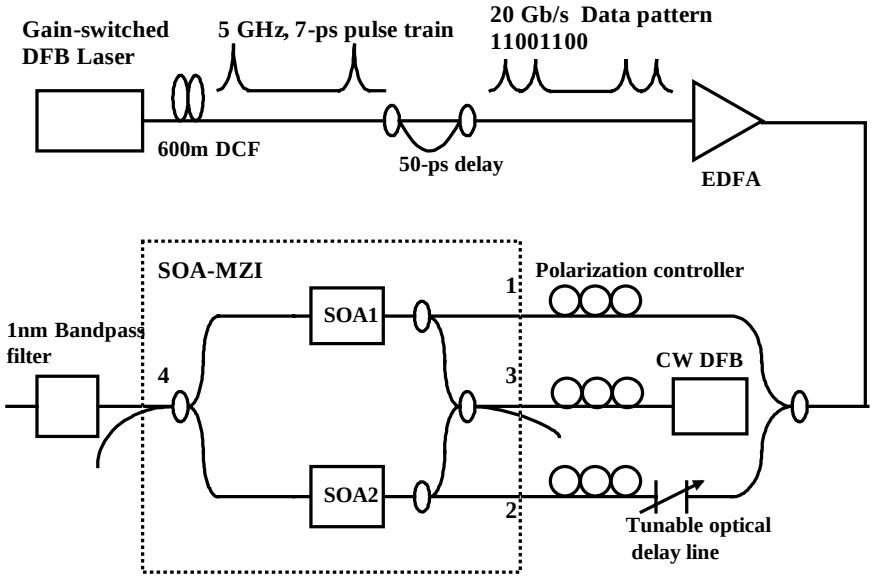


Figure 1: Experimental setup for demonstration all-optical XOR logic in SOA-MZI.

Figure 2 shows the results of the all-optical XOR logical gate operation. The top figure shows the results of a 20 Gb/s pattern and the bottom figure shows the results of a 40 Gb/s pattern. Figure 2(a) and Figure 2 (b) show the control signal A, "11001100…" and its 1 bit period delayed control signal B. The final XOR result is clearly seen in Figure 2 (c). However, the XOR output pulse is broad and pattern dependent, which is due to the long carrier recovery time of SOA in the SOA-MZI, and it is measured to be ~ 150 ps in our experiment for the 40 Gb/s case when the SOA`s are operated at high current.

For high speed all optical XOR logic operation with above scheme, fast carrier lifetime is required, and several methods have been proposed to reduce carrier lifetimes, however, nothing seemed to be considered feasible in satisfying speed and efficiency simultaneously [9]. An

efficient method to over come the limitation imposed by long carrier lifetime is using differential phase modulation scheme [9]. With differential phase modulation scheme, ultrahigh speed (>100 Gb/s) all optical processing, such as wavelength conversion [9,10], all optical demultiplexing [9] have been demonstrated with SOA based interferometer. All optical logic has been demonstrated using SOA `s configured as ultrafast nonlinear interferometer (UNI) [11]. We now report all-optical XOR logic gate based on the differential phase modulation scheme of a symmetrical

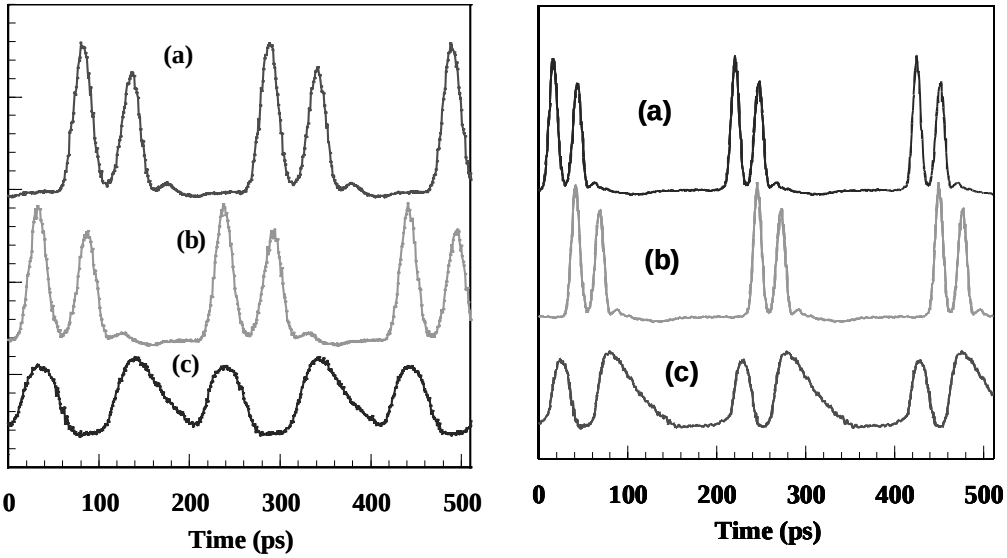


Figure 2: Left figure is for 20 Gb/s pattern and the right figure is for 40 Gb/s pattern. Output XOR at 1556 nm (a) Input data A (b) Input data B (c) XOR output

SOA-MZI [12,13]. The experiment is demonstrated at 10 Gb/s and 20 Gb/s with full duty cycle operation, and the pulse width of the XOR output is same as the input signal pulse width. The experimental arrangement and the principle are described in detail in Ref. [12, 13]. The results of a 20 Gb/s XOR experiment using a differential scheme is shown in Figure 3.

## SIMULATION

As shown in Figure 1 and Figure 3 (a), the CW light $P_{in}$ is divided and introduced via a 50:50 coupler into the two arms of the MZI. In the MZI, the control signals are launched into the two SOAs where they modulate the gain of the SOAs and thereby the phase of the co-propagating CW signal. At the output of the MZI, the CW light from the two SOAs interferes and the XOR output intensity can be described by the following basic interferometric equations:

$$P_{XOR}(t) = \frac{P_{in}}{4}\left\{G_1(t) + G_2(t) - 2\sqrt{G_1(t)G_2(t)}\cos\left[\phi_1(t) - \phi_2(t)\right]\right\}. \qquad (1)$$

In which, $G_{1,2}(t)$ is time dependent gain and $\phi_{1,2}(t)$ is phase shift in the two arms of SOA-MZI. The phase shift $\phi_{1,2}(t)$ is related to the gain $G_{1,2}(t)$ by the linewidth enhancement factor $\alpha$ and is given by:

$$\phi_1(t) - \phi_2(t) = -\frac{\alpha}{2}\ln\left(\frac{G_1(t)}{G_2(t)}\right) \tag{2}$$

The time dependent gain of the SOA satisfies the dynamical equation [16]:

$$\frac{d\ln(G_{1,2}(t))}{dt} = \frac{\ln G_0 - \ln G_{1,2}(t)}{\tau_c} - \frac{P_{1,2}(t)}{E_{sat}}(G_{1,2}(t) - 1) \tag{3}$$

where $\tau_c$ is the spontaneous carrier lifetime, $G_0$ is the unsaturated power gain and $E_{sat}$ is the saturation energy of the SOA. $P_{1,2}(t)$ is the instantaneous optical power inside the SOA1 and SOA2. We will consider scheme 1 at first. In the scheme 1, data A is coupled into SOA1 and data B is coupled into SOA2, so $P_{1,2}(t)$ can be expressed as following:

$$P_{1,2}(t) = P_{A,B}(t) + P_{CW}/2 \tag{4}$$

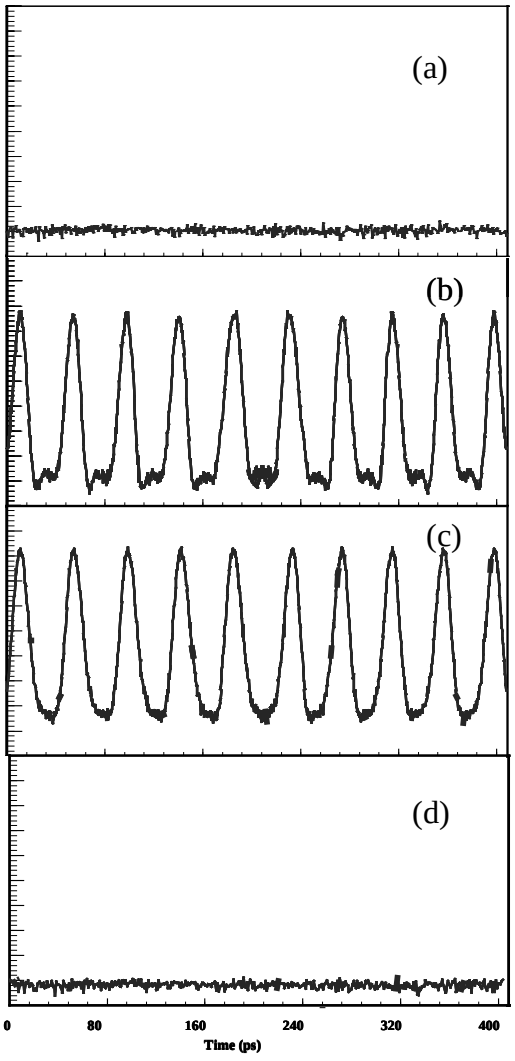

Figure 3: Output XOR at 1556 nm (a) A=0, B=0; (b) A=1, B=0; (c) A=0, B=1; (d) A=1, B=1. Rate = 20 Gb/s

In simulation, the data stream pulse is assumed to be Gaussian pulse with FWHM pulse width of 1/8 bit period, e.g. $\tau_{FWHM}=T/8$. so,

$$P_{A,B}(t)=\sum_{n=-\infty}^{+\infty}a_{nA,B}\frac{2\sqrt{\ln 2}P_0}{\sqrt{\pi}\tau_{FWHM}}\exp\left(-\frac{4\ln 2(t-nT)^2}{\tau_{FWHM}^2}\right) \qquad (5)$$

Where $P_0$ is the single pulse energy, $a_{nA,B}$ represents $n_{th}$ data in data stream A and B, $a_{nA,B}$= 1 or 0.

For a SOA based interferometric device, output pulse amplitude is decided by the maximum phase shift $\phi$ (as shown in Figure 4 (a)) induced by the control pulse. Figure 4(b) shows the relations between phase shift in one arm of the SOA-MZI and single pulse energy $P_0$ for different repetition rate, the parameters of the SOA are chosen as following, $G_0$=1000 and $\alpha$= 10. From Figure 4 we can see, the phase shift increases with increasing the single pulse energy, and it decreases with increasing control pulse rate. Phase shift of $\pi$ can be easily achieved when bit rate is low, e.g. single pulse energy $P_0$= .0025$E_{sat}$ can induce a phase shift of $\pi$ when bit period is same as carrier recovery time ($T=\tau_c$). In the high bit rate case, however, the phase shift becomes saturated with increasing $P_0$, e.g., when $T$=0.1 $\tau_c$, the phase shift becomes saturated when $P_0$ is larger than 0.01 $E_{sat}$, and the phase shift is only $\pi$/3. It is known that in an interferometric device, the larger the phase shift, the more sensitive the receiver.

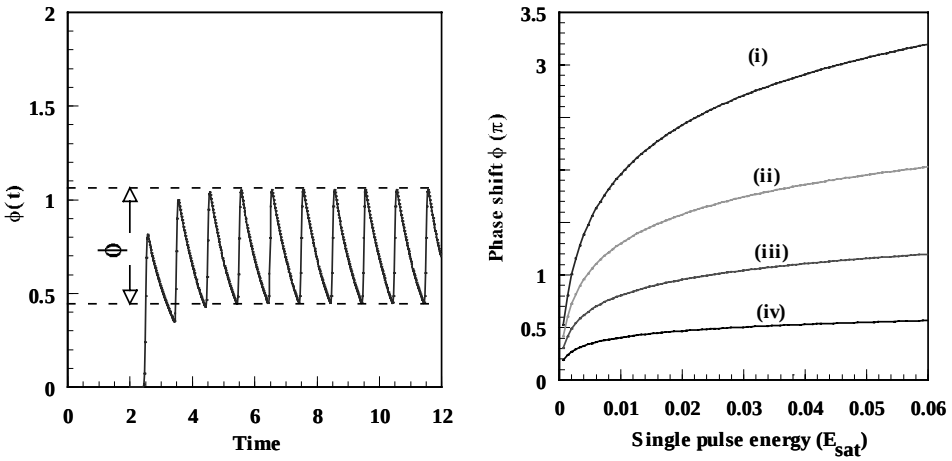


(a) (b)

Figure 4: Phase shift in one arm of the SOA-MZI induced by control signal (all "1"s) pulses (a) Evolution of the optical phase of the CW light (b) Relationship between maximum phase shift $\phi$ and single control pulse energy $P_0$ for different repetition rate (i) T= $\tau_c$, (ii) T= $\tau_c$/2, (iii) T= $\tau_c$/4, (iv) T= $\tau_c$/10

Figure 5 shows the output XOR of the SOA-MZI when a bit sequence is used in data stream A and data stream B at bit rate of $1/\tau_c$, $P_0$ =.0025$E_{sat}$ and $P_{CW}$ =0.01 $P_{sat}$ ($P_{sat}=E_{sat}/\tau_c$). It is clearly seen that the output XOR pulse is broader than the input signal pulse, and there is pattern effects. A deeper insight in the performance of the XOR logic can be gained by displaying the

superposition of repetition period long segments of the output XOR. These diagrams resemble the "classical" eye diagrams, but they are not as informative in the sense that degrading effects, normally observed in point-to-point communication links, such as noise sources added by the detector, optical fiber, etc. are absent. Nevertheless, theses diagrams, which will be called "pseudo-eye-diagrams" (PEDS) [17], are useful because, through isolation of the system from other effects, features of the operational principle of the analyzed device become evident. Following [17], quality factor

$$Q = \frac{P_1 - P_0}{\sigma_1 + \sigma_0} \qquad (6)$$

has been calculated in the diagrams to simplify the interpretation of the results where $P_1$ ($P_0$) and $\sigma_1$ ($\sigma_0$) are respectively, the average power and standard deviation of the XOR output 1s (0s).

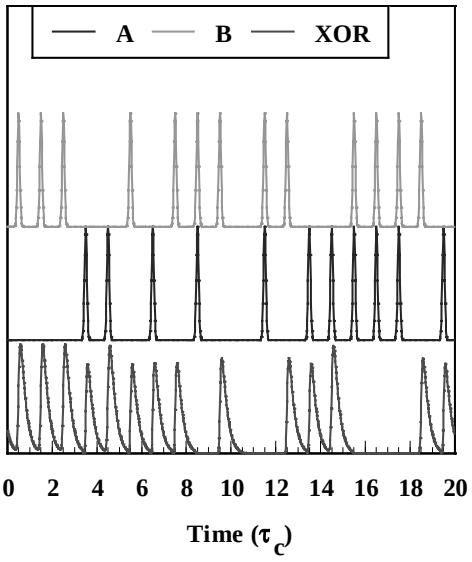


Figure 5: Sequence of XOR logic pattern produced at the output of SOA-MZI as a response to PRBS input at bit period T= $1/\tau_c$. CW input power is 0.02 $P_{sat}$, and the single pulse energy is 0.0025 $E_{sat}$.

Figure 6 presents the simulated PEDs of a "1"in the XOR output for 127 bit ( $2^7$-1) pseudorandom sequence of input pulses. The XOR output at bit rates of $1/\tau_c$, $2/\tau_c$, and $4/\tau_c$ are shown where $\tau_c$ is the gain recovery time. Q value decreases with increasing data bit rate, and the eye is closed at $4/\tau_c$. In the simulation, the single pulse energy is chosen as $0.01E_{sat}$ for the bit rate of $2/\tau_c$ and $4/\tau_c$ because the phase shift becomes saturated when $P_0 > 0.01E_{sat}$. For better performance of XOR in SOA-MZI, one method is to increase the power of the CW beam, so as to reduce carrier recovery time [18].

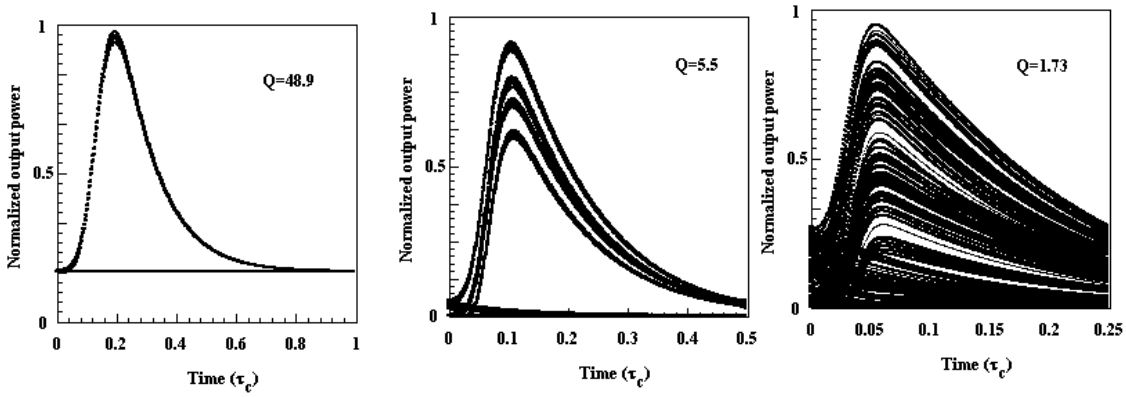


Figure 6: Simulated XOR output PEDs for different bit rates for non-differential scheme. $P_0$= $0.01E_{sat}$, and $P_{CW}$= 0.2 $P_{sat}$. (a) T= $\tau_c$, (b) T=0.5$\tau_c$ (c) T=0.25$\tau_c$

Similar calculations have been carried out for the differential scheme [13]. Results are shown in Figure 7.

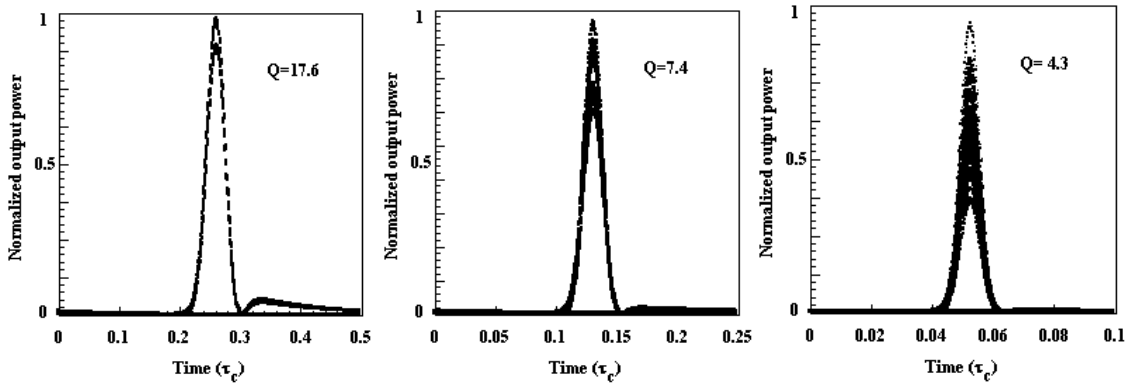


Figure 7: Simulated XOR output PEDs for different bit rates for differential scheme. $P_0$= $0.01E_{sat}$, and $P_{CW}$= 0.2 $P_{sat}$. (a) T= 0.5$\tau_c$, (b) T=0.25$\tau_c$ and (c) T=0.1$\tau_c$

## SUMMARY

All optical XOR functionality has been demonstrated experimentally using an integrated SOA-based Mach-Zehnder interferometer (SOA-MZI) at 20 Gb/s and 40 Gb/s. The performance of the XOR results has been analyzed by solving the rate equation of the SOA numerically. The high-speed operation is limited by the carrier lifetime in the SOA. In order to solve the limitations imposed by carrier lifetime, a differential phase modulation scheme for XOR operation has been proposed and experimentally investigated. Simulation shows that this scheme is potentially capable of XOR operation to > 100 Gb/s.

## REFERENCES


1. K. L. Hall and K. A. Rauschenbach, "All-optical bit pattern generation and matching ", Electron. Lett., vol. 32, pp.1214-1215, 1996.
2. A. J. Poustie, K. J. Blow, R. J. Manning, and A. E. Kelly, "All-optical pseudorandom number generator," Opt. Commun., vol. 159, pp.208-214, 1999.
3. T. Fjelde, A. Kloch, D. Wolfson, B. Dagens, A. Coquelin, I. Guillemot, F. Gaborit, F. Poingt, M. Renaud, "Novel scheme for simple label-swapping employing XOR logic in an integrated interferometric wavelength converter", IEEE Photon. Technol. Lett., vol. 13, pp.750-752, 2001
4. P. S. Naimish, K. L. Hall, and K. A. Rauschenbach, "Interferometric all-optical switches for ultrafast signal processing", Applied Optics, vol. 37, pp.2831-2842, 1998
5. M. Jinno, and T. Matsumoto, "Ultrafast all-optical logic operations in a nonlinear sagnac interferometer with two control beams", Opt. Lett., vol. 16, pp.220-222 (1991)
6. T. Houbavlis, K. Zoiros, A. Hatziefremidis, H. Avramopoulos, L. Occhi, G. Guekos, S. Hansmann, H. Burkhard and R. Dall'Ara, "10 Gbit/s all-optical Boolean XOR with SOA fiber Sagnac gate", Electron. Lett., vol. 35, pp.1650-1652,1999
7. C. Bintjas, M. Kalyvas, G. Theophilopoulos, T. Stathopoulos, H. Avramopoulos, L. Occhi, L. Schares, G. Guekos, S. Hansmann, and R. Dall'Ara, " 20 Gb/s all-optical XOR with UNI gate", IEEE Photon. Technol. Lett., vol. 12, pp.834-836, 2000
8. T. Fjelde, D. Wolfson, A. Kloch, B. Dagens, A. Coquelin, I. Guillemot, F. Gaborit, F. Poingt, and M. Renaud, "Demonstration of 20 Gbit/s all-optical logic XOR in integrated SOA-based interferometric wavelength converter", Electron. Lett., 2000, 36 (22), pp. 1863-1864
9. K. Tajima, S. Nakamura, and Y. Ueno, "Ultrafast all-optical signal processing with Symmetric Mach-Zehnder type all-optical switches", Optical and Quantum Electronics, vol. 33, pp. 875-897, 2001
10. J. Leuthold, C. Joyner, B. Mikkelsen, G. Raybon, J. Pleumeekers, B. Miller, K. Dreyer, and C. Burrus, "100 Gbit/s all-optical wavelength conversion with integrated SOA delayed-interference configuration", Electron. Lett., vol. 36, pp.1129-1130, 2000
11. K. L. Hall, and K. A. Rauschenbach, " 100-Gbit/s bitwise logic", Opt. Lett., vol. 23, pp.1271-1273, 1996
12. H. Chen, G. Zhu, J. Jaques, J. Leuthold, A. B. Piccirilli, N. K. Dutta, "All-optical logic XOR using a differential scheme and Mach-Zehnder interferometer" Electronics Lett. Vol. 38, 1271-1273, 2002
13. Q. Wang, G. Zhu, H. Chen, J. Jaques, J. Leuthold, A. B. Piccirilli, N. K. Dutta " Study of All-Optical XOR Using Mach-Zehnder Interferometer And Differential Scheme" IEEE, JQE, vol. 40, 703-710, June 2004
14. R. J. Manning and G. Sherlock " Recovery of $\pi$ phase shift in ~ 12.5 ps in a semiconductor laser amplifier" Electronics Lett. Vol 31, 307-308, 1995
15. R. J. Manning, D.A.O. Davies, D. Cotter and J. K. Lucek " Enhanced recovery rates in semiconductor laser amplifiers using optical pumping " Electronics Lett. Vol 30, 787-788, 1994
16. G. P. Agrawal and N. A. Olsson, IEEE J. Quantum Electron., vol. 25, pp.2297-2306,1989
17. R. Gutierrez-Castrejon, L. Occhi, L. Schares, and G. Guekos, "Recovery dynamics of cross-modulated beam phase in semiconductor amplifiers and applications to all-optical signal processing", Optics Communications, vol. 195, pp167-177
18. F. Girardin, G. Guekos, and A. Houbavlis, " Gain recovery of bulk semiconductor optical amplifiers", IEEE Photon. Lett., vol. 10, pp.784-786